Lack of cAMP-response Element-binding Protein 1 in the Hypothalamus Causes Obesity*◻️S

Franck Chiappini, Lucas L. Cunha, Jamie C. Harris, and Anthony N. Hollenberg[1]

From the Division of Endocrinology, Diabetes and Metabolism, Beth Israel Deaconess Medical Center and Harvard Medical School, Boston, Massachusetts 02215

The melanocortin system in the hypothalamus controls food intake and energy expenditure. Its disruption causes severe obesity in mice and humans. cAMP-response element-binding protein 1 (CREB1) has been postulated to play an important role downstream of the melanocortin-4 receptor (MC4R), but this hypothesis has never been confirmed *in vivo*. To test this, we generated mice that lack CREB1 in *SIM1*-expressing neurons, of the paraventricular nucleus (PVN), which are known to be MC4R-positive. Interestingly, CREB1$^{\Delta SIM1}$ mice developed obesity as a result of decreased energy expenditure and impairment in maintaining their core body temperature and not because of hyperphagia, defining a new role for CREB1 in the PVN. In addition, the lack of CREB1 in the PVN caused a reduction in vasopressin expression but did not affect adrenal or thyroid function. Surprisingly, MC4R function tested pharmacologically was normal in CREB1$^{\Delta SIM1}$ mice, suggesting that CREB1 is not required for intact MC4R signaling. Thus CREB1 may affect other pathways that are implicated in the regulation of body weight.

The melanocortin 4 receptor (MC4R)[2] is widely expressed in the central nervous system, including a number of sites that contribute to coordinated control of body weight (1–3). The essential role of the MC4R is evident from the presence of severe obesity in both MC4R knock-out mice and in humans with naturally occurring mutations (4, 5). These mutations cause increased food intake and decreased energy expenditure

(4, 6, 7). One key site of MC4R expression is the paraventricular nucleus of the hypothalamus (PVN) (1–3). The PVN is an area that regulates several neuroendocrine, behavioral, and autonomic functions, especially food intake and energy expenditure (8–11). It has been implicated in the regulation of body weight as re-expression of MC4R in the PVN of mice on a null background rescues the obese phenotype (12). Mutations in the *SIM1* (single-minded 1) gene, a transcription factor that controls development of the PVN, lead to the development of obesity in humans and mice, further implicating the PVN as a key regulator of body weight (13–17).

The MC4R is known to signal through $G_s\alpha$, which in turn activates adenylyl cyclase, leading to increased intracellular levels of cAMP (1, 3, 18). Elevated cAMP levels induce phosphorylation and activation of the transcription factor cAMP-response element-binding protein (CREB1) through increased activity of protein kinase A, or PKA (19–22). The importance of this pathway in body weight regulation *in vivo* is highlighted by the fact that constitutive activation of PKA is associated with leanness (23). The phosphorylation of CREB1 leads to the activation of CREB target gene expression (24, 25). CREB signaling is complicated by the fact that a number of related transcription factors including cAMP-response element modulator (CREM) and activating transcription factor 1 are also phosphorylated by PKA and can compensate for CREB1 in its absence. Although activating transcription factor 1 is not thought to be expressed in the murine brain, CREM is known to be up-regulated when CREB1 is deleted. It is likely that both CREB1 and CREM have overlapping yet distinct roles in regulating target gene expression (26–31).

Once phosphorylated, CREB1 recruits a coactivator complex that includes CREB-binding protein and p300 to induce gene expression (21). Recently, CREB1 has been shown to require another specific family of coactivator proteins termed CRTCs (CREB-regulated transcriptional coactivators) (32). Interestingly CRTC1 KO mice develop obesity, whereas CRTC2 is implicated in glucose homeostasis (33, 34).

Activation of MC4R has been shown to phosphorylate CREB1 *in vitro* (35, 36). Thus CREB1 is postulated to mediate the genomic actions of MC4R *in vivo* (37), but this has not been previously tested. To do this, we used the *Cre/loxP* system and were able to delete CREB1 specifically in the PVN, the supra optic nucleus (SON), the nucleus of the lateral olfactory tract (NLOT), and the medial amygdala (MeAD) by using mice that express the *Cre*-recombinase in SIM1 expressing neurons (*SIM1^{Cre}* mice). Our data demonstrate that CREB1$^{\Delta SIM1}$ mice develop obesity on both chow and high fat diets. This appears to

[1] To whom correspondence should be addressed: 330 Brookline Ave., E/CLS 0728, Boston, MA 02215. Tel.: 617-735-3268; Fax: 617-735-3323; E-mail: thollenb@bidmc.harvard.edu.

[2] The abbreviations used are: MC4R, melanocortin-4 receptor; ACC1, acety-CoA carboxylase 1; ADRB1, β-adrenergic receptor 1; AVP, [Arg⁸]-vasopressin; BAT, brown adipose tissue; CBT, core body temperature; CE, cold exposure; CREB1, cAMP-response element binding protein; CREM, cAMP-response element modulator; DIO2, deiodinase 2; GTT, glucose tolerance test; GMPr, guanosine monophosphate receptor; HFD, high fat diet; ITT, insulin tolerance test; MeAD, medial amygdale; MT II, melanotan II; NLOT, nucleus of the lateral olfactory tract; OXT, oxytocin; PGC1, peroxisome proliferator-activated receptors gamma coactivator 1; PKA, protein kinase A; PVN, paraventricular nucleus of the hypothalamus; SON, supra optic nucleus; TRH, thyrotropin-releasing hormone; UCP1, uncoupling protein 1; WT, wild-type.

be mediated by a decrease in energy expenditure and an impairment in maintaining their core body temperature, despite the increase in CREM expression in hypothalamic areas where CREB1 is absent. Surprisingly, MC4R signaling is not impaired in these animals. The global function of the hypothalamic-pituitary-thyroid and hypothalamic-pituitary-adrenal axes are also unchanged. However, vasopressin expression is decreased in the PVN of $CREB1^{\Delta SIM1}$ mice. Taken together these data suggest that CREB1 plays a specific role in body weight regulation via modulation of energy expenditure through downstream genomic targets.

EXPERIMENTAL PROCEDURES

Generation of $CREB1^{\Delta SIM1}$ Mice

To generate specific CREB1 knock-out ($CREB1^{\Delta SIM1}$) mice, mice harboring the $CREB1^{loxP/+}$ allele (C57BL6, a gift of Dr. G. Schutz) were crossed with $SIM1^{Cre}$ transgenic mice (mixed C57Bl6, 129Sv, and FVB background) that express *Cre-recombinase* specifically in the PVN, medial amygdala, the SON, and the NLOT (12, 28, 38). The $CREB1^{loxP/+} \times SIM1^{Cre}$ mice obtained from this first breeding were crossed with the $CREB1^{loxP/+}$ mice to obtain a second generation containing control mice (WT, $CREB1^{loxP/loxP}$, and $SIM1^{Cre}$ littermates) and $CREB1^{\Delta SIM1}$ mice. *Cre*-mediated recombination of the $CREB1^{loxP/loxP}$ exon 10 allele leads to a null allele that encodes a truncated unstable protein devoid of DNA-binding and dimerization domains. Thus the result is the loss of CREB1 (12, 28). To obtain the second cohort of mice maintained at 18 °C, the same breeding scheme was used. Analysis of variance testing in both cohorts across different parameters has shown no differences between the three groups of controls: wild-type, $SIM1^{Cre}$, and $CREB1^{loPx/loxP}$ (littermates). For the third cohort we used the following breeding scheme $CREB1^{loxP/loxP} \times CREB1^{\Delta SIM1}$ to obtain $CREB1^{loxP/loxP}$ littermates and $CREB1^{\Delta SIM1}$ mice.

Analysis of $CREB1^{\Delta SIM1}$ Mice

A first cohort of mice (WT, $CREB1^{loxP/loxP}$, $SIM1^{Cre}$, and $CREB1^{\Delta SIM1}$) were housed individually at 22–24 °C using a 12 h of light/12 h of dark cycle with chow food (Harlan Teklad) and water provided *ad libitum*. A second cohort of mice ($CREB1^{loxP/loxP}$ and $CREB1^{\Delta SIM}$) was housed individually at 18 °C (long mild-cold exposure) with the same diet conditions as above. Finally, a third cohort ($CREB1^{loxP/loxP}$ and $CREB1^{\Delta SIM}$) of mice was housed under the same conditions above at 22–24 °C on a high fat diet (60% kCal fat, #D12492i; Research Diets). Body weight and food intake were recorded weekly. The mice were euthanized by decapitation to measure serum corticosterone level or by CO_2 inhalation. All of the experiments were approved by the Institutional Animal Care and Use Committee of Beth Israel Deaconess Medical Center.

Immunohistochemistry

The brains were cut in coronal 30-μm sections. Sections containing the PVN were from bregma -0.58 to -1.22 mm. Immunohistochemistry methods have been described previously (39). The following primary antibodies were used: polyclonal total anti-CREB1 (1:200; Cell Signaling Technology), polyclonal anti-CREM (1:50; Santa Cruz Biotechnology), anti-oxytocin (OXT) and anti-[Arg^8]-vasopressin (AVP; 1:500, Peninsula Laboratories). Secondary antibody rabbit IgG and diaminobenzidine kits were used (Vector Laboratories, Inc.). Immunohistochemistry analysis and quantification methods have been established previously (40). Specifically, this technique has been used to quantify neuropeptides including OXT and AVP (41–43).

Nissl Staining

The sections were delipidated in 1:1 alcohol/chloroform overnight and then rehydrated with decreasing concentrations (100 –95, 60, and 30%) of ethanol to distilled water. The sections were stained in 0.1% cresyl violet solution for 3–5 min and destained with a solution containing 44 ml of 95% of alcohol, 66 ml of chloroform, and nine drops of glacial acetic acid. They were then dehydrated through increasing concentrations (30, 60, and 95–100%) ethanol for 3 min each and cleared with xylene for 3 min (44).

Body and Blood Composition

Body Composition—To determine the body composition of mice two different methods were used: 1) magnetic resonance imaging with EchoMRI^{TM} (Echo Medical System) and 2) PIXImus dual-energy x-ray absorptiometer with software version 1.2 (GE Healthcare).

Blood Tests—Fed mice were euthanized between 8 and 10 a.m., and blood and tissue were collected. Serum was extracted and assayed for insulin (Crystal Chem.), leptin (R & D Systems Inc.), and corticosterone levels (Immunodiagnostic Systems Ltd.). Radioimmunoassay was used for total T4 and total T3 measurements (Coat-A-Count, Siemens). Blood glucose was assessed by One Touch Ultra glucometer (LifeScan, Inc.).

Thyrotropin-releasing Hormone (TRH) In Situ Hybridization

To determine the expression of *TRH* mRNA *in situ* hybridization was performed as described previously (39, 45). Briefly, the images were acquired on Zeiss Axioimager. A1 with Axiovision 4.8 software (Oberkochen, Germany). Dark-field digital images of each hypothalamic region of the brain were taken with the same exposure time, brightness, and contrast. The images were quantified using ImageJ (Public Domain, Developed at the National Institute of Mental Health, Bethesda, MD). The same threshold was used for comparison sets. The total number of positive pixels/unit area (pixel density) was calculated subtracting background from areas not expressing TRH mRNA. Pixel density in each region of the hypothalamus was averaged from a minimum of three matching sections of the PVN. The data represent the average pixel density $\pm$ S.E.

Analysis of the MC4R Pathway

Expression of MC4R mRNA by In Situ Hybridization—*In situ* hybridization for mouse *MC4R* mRNA was performed as described above (1, 12).

MC4R Signaling—To test the functionality of the MC4R pathway, we performed two tests using the MC3/4-R agonist
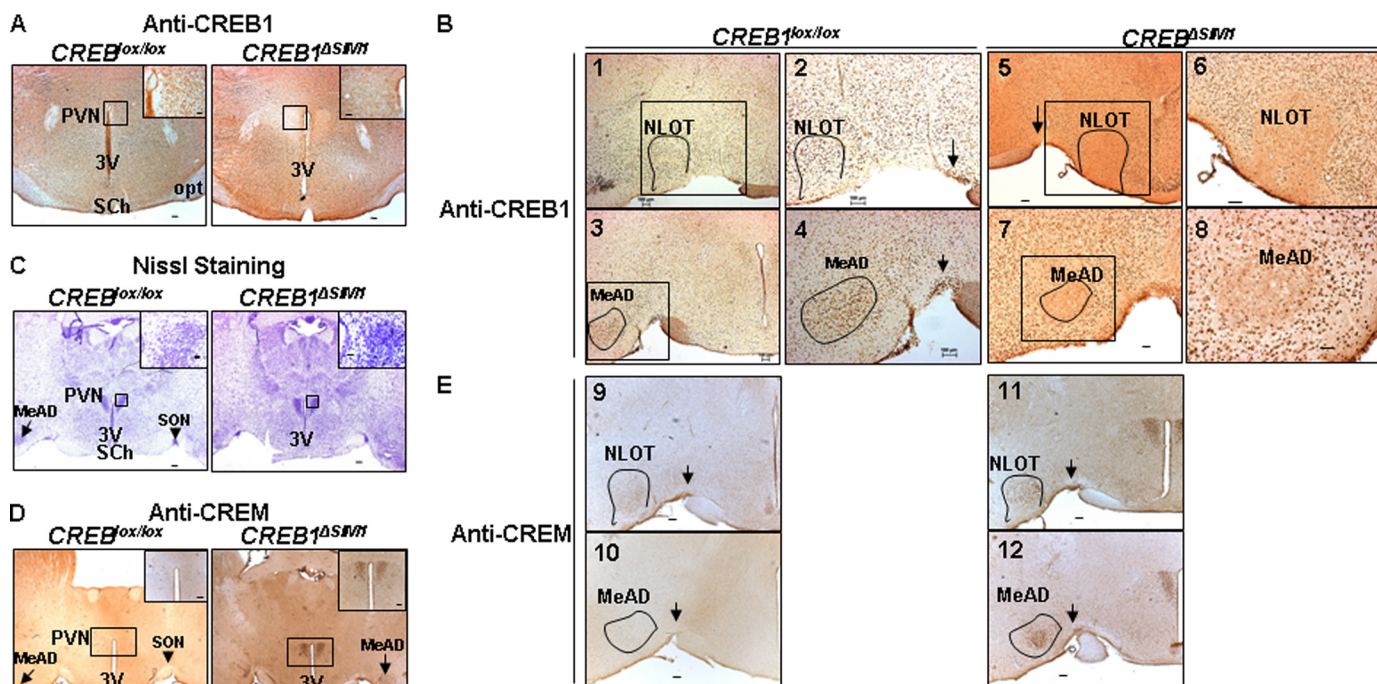
FIGURE 1. **CREB1$^{\Delta SIM1}$ mice overexpress CREM in the PVN, SON (arrows), NLOT, and MeAD.** *A* and *B*, immunohistochemistry against CREB1 in *CREB1$^{lox/lox}$* and *CREB1$^{\Delta SIM1}$* mice detailing the PVN and third ventricle (*3V*) (*A*) and detailing the SON, NOLT, and MeAD (*black boxes*) (*B*). In *B*, *panels 1, 3, 5*, and *7* are at 5× magnification. The highlighted areas, shown in *panels 2, 4, 6*, and *8* are at 10× magnification. *C*, Nissl staining was performed in the same mice. *D* and *E*, immunohistochemistry against CREM was performed in the same mice as detailing the PVN and third ventricle and detailing the SON (*arrow*), NLOT, and MeAD (*E*). *SCh*, suprachiasmatic nucleus. *Bar scale*, 100 μm. Shown are representative images from a total of four animals/group.

melanotan II (MT II) and the MC4R-specific agonist Ro27-3225. Briefly, on day 1, single-caged mice were fasted for 12 h. 30 min prior to the start of the dark cycle, the food was returned, and the mice were injected intraperitoneally with 200 μl of saline (0.9% sodium chloride injection; USP, Hospira Inc.). Food intake was measured for 3.5 h following the injection. On day 2, the same mice were fasted for 12 h. 30 min prior to the start of the dark cycle, the food was returned, and the mice were injected with 100 μg of MT II (H-3902; Bachem)/mouse in 200 μl of saline 30 min before the start of the dark cycle. Again, food intake was measured for 3.5 h (6, 12). The same protocol was used to test Ro27-3225 (Sigma) at 6.6 mg/kg. As each mouse served as its own control, a paired *t* test was used to analyze these data (6, 12, 46).

Energy Expenditure and Core Body Temperature (CBT)

Indirect Calorimetry—The metabolic rates were measured by indirect calorimetry in 12–14-week-old female *CREB1$^{\Delta SIM1}$* and control mice (from the mice housed at 18 °C) by using the 16-chamber open-circuit Oxymax system of the comprehensive laboratory animal monitoring system; Columbus Instruments) and following a previously published protocol (12, 47).

Cold Exposure and CBT—The same group of mice used for indirect calorimetry was then used for the cold challenge. To determine the normal CBT of mice, we used a rectal probe (Physitemp Instruments Thermalert Model TH-8, Inc.). CBT readings were taken twice daily (8:00 a.m. and 8:00 p.m.) for three consecutive days. The mean for each animal per time point was averaged from the three days. The results are displayed as the means ± S.E. per genotype per time point. During the cold challenge at 4 °C, the

CBT of each animal was monitored every hour over a 7-h period. Body weight and the food intake were recorded at the beginning and end of the experiment.

Intraperitoneal Glucose Tolerance Test (GTT) and Insulin Tolerance Test (ITT)

GTT—Male and female *CREB1$^{\Delta SIM1}$* and control mice were fasted for 16 h prior to the start of the intraperitoneal GTT. After a sample of fasted blood (time 0) was collected, the animals were given glucose (1 g/kg of body weight, 20% dextrose; Baxter) intraperitoneally. Blood glucose readings were then taken at 15, 30, 60, 120, and 180 min.

ITT—For the ITT, the same mice were fasted for 6 h. After a sample of fasted blood was collected (time 0), the animals were injected intraperitoneal with Humulin R (Eli Lilly and Co.). Blood glucose readings were then taken after 15, 30, 60, 120, and 180 min using the One Touch Ultra (LifeScan, Inc.).

Real Time Quantitative PCR

Total mRNA was extracted from brown adipose tissue with the RNA-STAT-60 kit and quantified with the NanoDrop®-ND1000 (Thermo Scientific). cDNA was obtained by using the Advantage® RT-for-PCR kit (Clontech Laboratories Inc.). To quantify *UCP1* (uncoupling protein 1), *PGC1α* (peroxisome proliferator-activated receptors γ coactivator 1), *DIO2* (deiodinase 2), *ADRB1* (β-adrenergic receptor), *ACC1* (acety-CoA carboxylase 1), and *GMPr* (guanosine monophosphate receptor) gene expressions, TaqMan® assays were used (Mm00494069_m1, Mm01208835_m1, Mm00515664_m1, Mm00431701_s1, Mm01304277_m1, and Mm00499395_m1,

respectively) (Applied Biosystems). *Cyclophilin* was used as a control. Quantitative PCR was run using the Stratagene® MX3000P® (Agilent Technologies). The gene to *cyclophilin* ratio was calculated for each sample based on the arbitrary value of copies determined by the standard curve for each gene.

Western Blotting

50 mg of brown adipose tissue from mice was homogenized in 1 ml of lysis buffer (Cell Signaling Technology) containing protease and phosphatase inhibitors using a TissueLyser (Qiagen) for 1 min at 30 Hz. The homogenates were centrifuged at $16,000 \times g$ for 20 min at 4 °C, and the supernatant was transferred to a fresh tube. The proteins were resolved using 10% NuPAGE bis-tris gels (Invitrogen) and transferred to nitrocellulose membranes. The blots were probed for UCP1 (anti-UCP1, 1:200; Santa Cruz Biotechnology Inc.) and visualized using the ECL-Plus kit (Amersham Biosciences™ GE Healthcare). For actin, the blots used to detect UCP1 were stripped and reprobed for actin (anti-actin, 1:1000; Sigma).

Plasmid Construction

To construct pGL3-*avp-luc*, -2009 to $+27$ of the putative mouse *avp* promoter was PCR-amplified from BAC RP24–388N9 (forward primer, CTCTGGTGGACATGCCACTC; reverse primer, GCAGCA**GCTAGC**CCGTAGTGTTGAGCA-TCCTGGC; an added NheI restriction enzyme site is shown in bold type) and cloned into pGL3-basic (Promega) using KpnI-NheI sites and sequenced.

Cell Culture and Transient Transfection

293T cells were transfected in six-well plates with 10 ng of a CMV-β-galactosidase expression vector and 50 ng of a pGL3-*avp-luc* or pGL3 alone to determine the response to cAMP. To determine the response to CREB and CREM, 293T cells were transfected with the above reporters and 50 ng of either pKCR2-CREB (35, 36), pKCR2-CREMα, or pCDNA3.1-CREMτ2 (CREM plasmids are a generous gift from Dr. P. Sassone-Corsi) as indicated. pGL3-*avp-luc* was also cotransfected with pKCR2 and pCDNA3.1 alone. All of the transfections were performed with Lipofectamine™ 2000 (Invitrogen) in serum-free OptiMem medium (Invitrogen). Sixteen hours after transfection, the cells were treated with or without 8-bromo-cAMP (250 μM) for 8 h. The cells were lysed and assayed for luciferase and β-galactosidase activity, respectively. All of the transfections described were performed in triplicate. The data shown are the means $\pm$ S.E. of at least three separate experiments.

Statistical Methods

All of the data are presented as the means $\pm$ S.E. To test for differences between groups of mice an analysis of variance test was run followed by a post hoc test Bonferonni adjustment. The data sets were analyzed using a two-tailed unpaired Student's *t* test. For the MT II and Ro27-3225 tests and the cold challenge experiments, a two-tailed paired Student's *t* test was run as each mouse served as its own control. Type one error α was set at 5% for all of our statistical analysis.
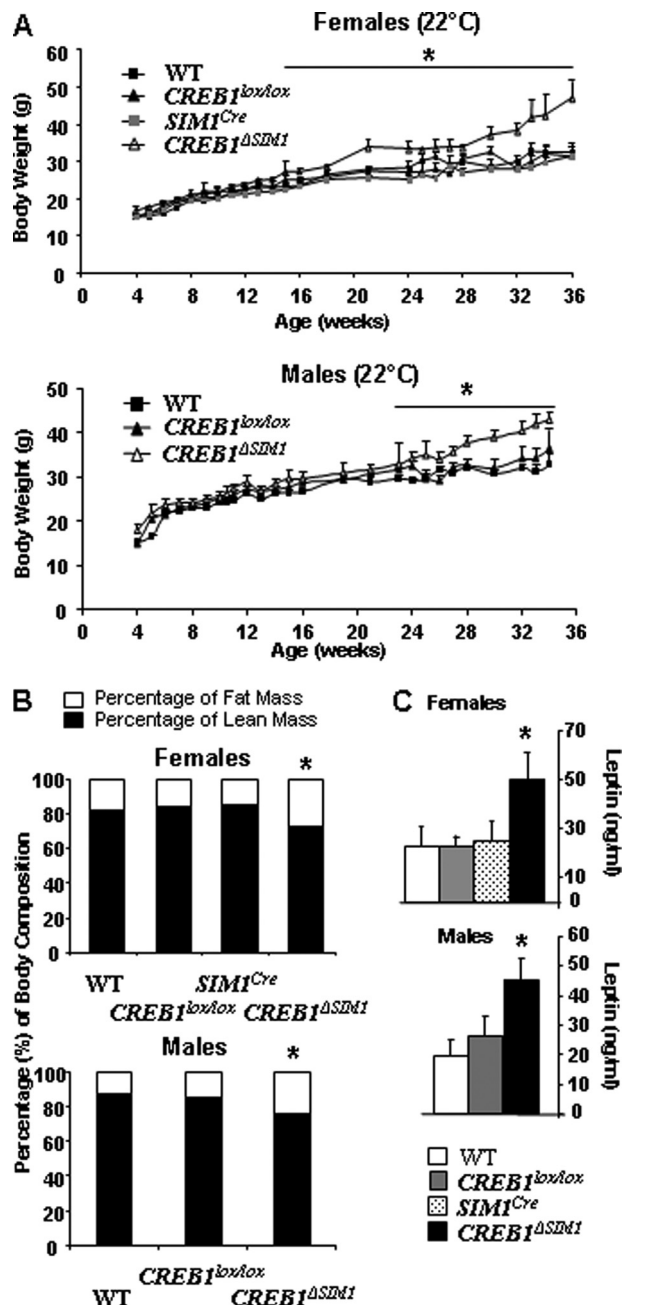

FIGURE 2. **CREB1$^{\Delta SIM1}$ mice have an increase in body weight, fat mass, and serum leptin levels on a chow diet.** *A*, body weight in females and males. *B*, body composition by magnetic resonance imaging (percentage of lean and fat mass) in females and males. *C*, serum leptin levels in females and males. The data are represented as the means $\pm$ S.E. *, $<p = 0.05$. For n = males/females: WT, $n = 10/8$; *CREB1$^{lox/lox}$*, $n = 12/12$; *SIM1^{Cre}*, $n = 6$ females; *CREB1$^{\Delta SIM1}$*, $n = 11/13$. The mice were housed at 22 °C.

RESULTS

Generation of Mice Lacking CREB1 in the Paraventricular Nucleus—To generate mice that lack CREB1 in the PVN, we crossed transgenic mice expressing *Cre*-recombinase under the control of SIM1 regulatory elements with mice possessing a conditional CREB1 allele (12, 28). As shown in Fig. 1*A*, *CREB1$^{\Delta SIM1}$* mice do not express CREB1 in the PVN. The *CREB1$^{\Delta SIM1}$* mice also lack expression of CREB1 in other areas known to express *SIM1* including the NLOT (Fig. 1*B*), SON (Fig. 1*B*), and MeAD (Fig. 1*B*). Because the deletion of the mem-
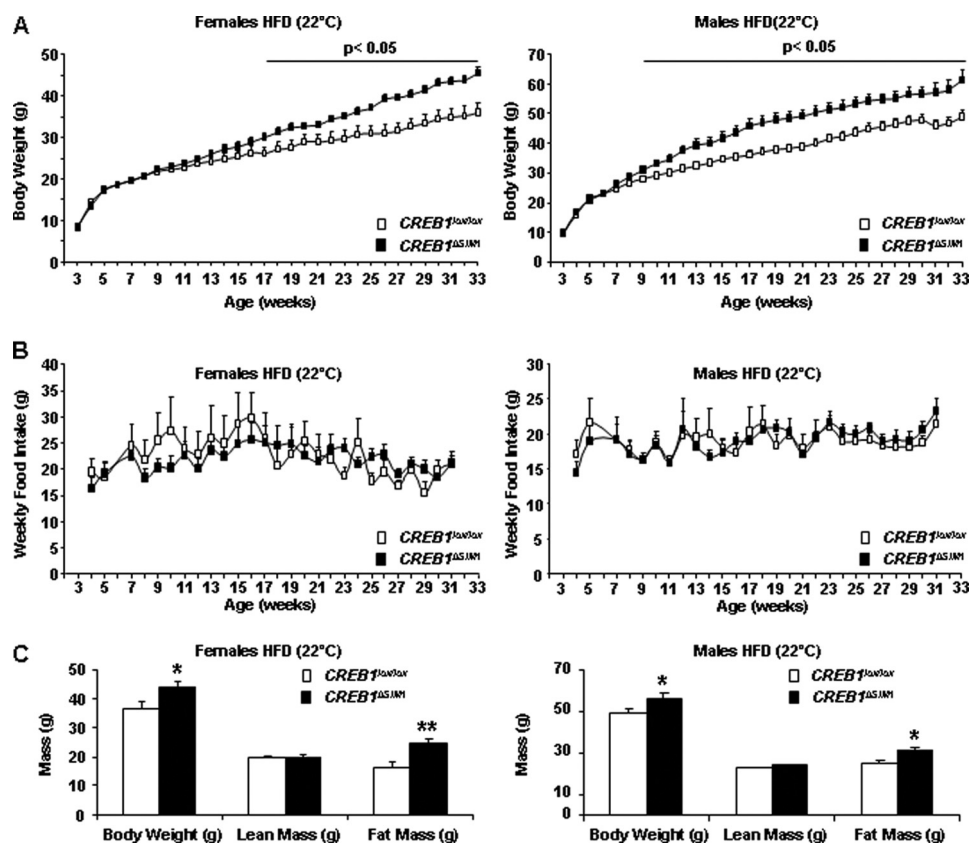
FIGURE 3. **CREB1$^{\Delta SIM1}$ mice develop obesity on a HFD.** *A,* body weight in control and *CREB1*$^{\Delta SIM1}$ mice. *B,* food intake in control and *CREB1*$^{\Delta SIM1}$ mice. *C,* body composition (dual-energy X-ray absorptiometer) in control and *CREB1*$^{\Delta SIM1}$ mice. The mice were 33 weeks old. A group of male and female mice was fed with high fat diet and held at 22 °C. For *n* = males/females: *CREB1*$^{lox/lox}$, *n* = 14/10; *CREB1*$^{\Delta SIM1}$, *n* = 10/15. *, *p* < 0.05; **, *p* < 0.01.

bers of the CREB family can induce neuronal apoptosis, we verified the integrity of the areas that lack CREB1, using Nissl staining and did not see evidence of neuronal loss (Fig. 1*C*). CREM, a member of the CREB family, can compensate for CREB1 in its absence. Therefore, we examined CREM expression by immunohistochemistry and found it to be up-regulated in areas where CREB1 is deleted (Fig. 1, *D* and *E*), further confirming the integrity of these neurons. Thus mice lacking CREB1 in SIM1 neurons (27) are a viable model to examine the role of CREB1 *in vivo*.

The Lack of CREB1 Leads to Obesity—To test the role of CREB1 *in vivo*, we followed the body weight of male and female *CREB1*$^{\Delta SIM1}$ mice and their respective controls on chow diet in the first cohort housed at 22 °C. As is shown in Fig. 2*A*, the body weights of male and female *CREB1*$^{\Delta SIM1}$ mice are increased beginning at 22 weeks and 16 weeks of age, respectively, and this is associated with a significant increase in body fat content and serum leptin levels (Fig. 2, *B* and *C*). We also looked for indications of glucose intolerance in male and female *CREB1*$^{\Delta SIM1}$ mice. Once the mice were obese, we found evidence of glucose intolerance in male *CREB1*$^{\Delta SIM1}$ mice but not in female mice as demonstrated by a GTT (supplemental Fig. S1*A*). Also, male *CREB1*$^{\Delta SIM1}$ mice have a significant increase in serum insulin in the fed state (supplemental Fig. S1*C*), with no change in blood glucose (supplemental Fig. S1*D*). However, the ITT is normal in both male and female *CREB1*$^{\Delta SIM1}$ mice compared with controls (supplemental Fig. S1*B*). ITTs and GTTs were also performed in the same group of mice on a chow

diet at 8–10 and 16–18 weeks of age. No difference was observed between the control groups and the *CREB1*$^{\Delta SIM1}$ mice (data not shown).

A second group of male and female *CREB1*$^{\Delta SIM1}$ mice on a HFD also became obese (Fig. 3*A*). There was no difference in food intake in male and female *CREB1*$^{\Delta SIM1}$ mice on the HFD (Fig. 3*B*), suggesting that the development of obesity is secondary to decreased energy expenditure. Lean and fat mass were measured in these mice at 33 weeks of age, and male and female *CREB1*$^{\Delta SIM1}$ mice have similar lean mass (Fig. 3*C*) but increased fat mass (Fig. 3*C*) compared with control mice. Despite the development of obesity in *CREB1*$^{\Delta SIM1}$ mice on a HFD, both GTTs and ITTs at 28–29 weeks of age (and earlier time points) are not different from controls (supplemental Fig. S2).

CREB1$^{\Delta SIM1}$ *Mice Have Lower Energy Expenditure and Are Cold-intolerant*—Mice lacking CREB1 in the PVN, SON, NLOT, and MeAD develop obesity on chow and HFD, with normal food intake indicative of decreased energy expenditure. However, we next noticed that when genetically identical kindred were housed at a lower temperature of 18 °C, male and female *CREB1*$^{\Delta SIM1}$ mice are significantly leaner than controls early in life (Fig. 4*A*) but then converge to controls by 11 weeks of age for males and 18 weeks of age for females. When transferred to a warmer environment (22 °C) for comprehensive laboratory animal monitoring system analysis, these mice demonstrated decreased oxygen consumption and significantly lower respiratory exchange ratio and heat production (Fig. 4*B*), indi-
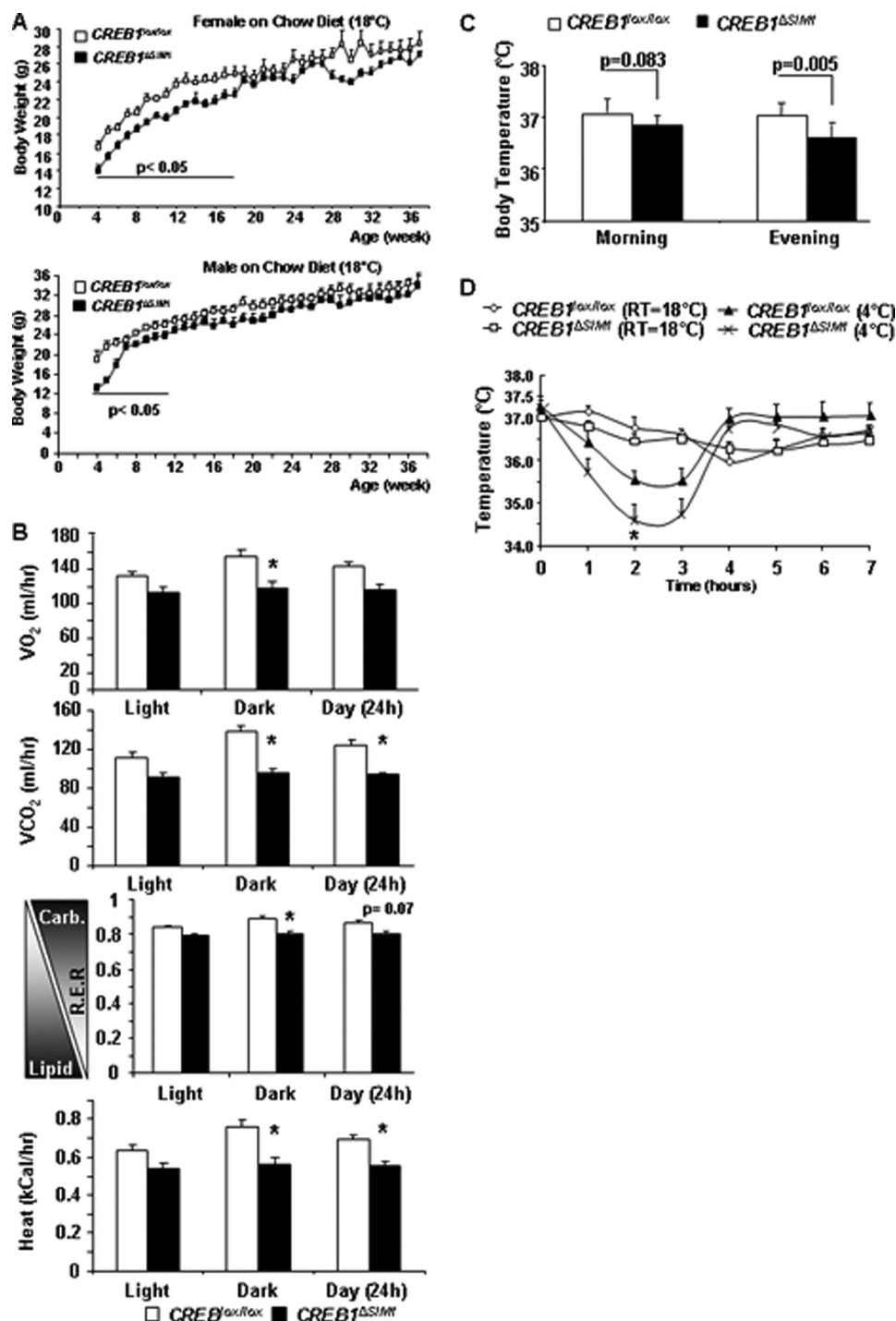
FIGURE 4. **CREB1$^{\Delta SIM1}$ mice housed at 18 °C have decreased body weight.** *A*, body weight of mice fed a normal chow diet and housed at 18 °C (second cohort). For *n* = males/females: *CREB1$^{lox/lox}$*, *n* = 8/8; *CREB1$^{\Delta SIM1}$*, *n* = 8/9. *B*, comprehensive laboratory animals measurement system was performed in the female *CREB1$^{lox/lox}$* and *CREB1$^{\Delta SIM1}$* mice (14 weeks old; *n* = 8/group) housed at 18 °C. The comprehensive laboratory animal monitoring system room was maintained at 22 °C. *R.E.R.*, respiratory exchange ratio = VO_2/VCO_2. *C*, core body temperature in *CREB1$^{lox/lox}$* and *CREB1$^{\Delta SIM1}$* mice at room temperature (18 °C) in the morning (8:00 a.m.) and the evening (7:00 p.m.). *D*, core body temperature for 7 h at room temperature on day 1 (18 °C) and during cold exposure on day 2 (4 °C). *, *p* = 0.03. The data are represented as the means ± S.E. *, *p* < 0.05. At room temperature 18 °C, *n* = 8 mice/group; during cold exposure 4 °C; *n* = 7–8 mice/group. As each mouse is its own control, a paired *t* test was used to analyze these data. *, *p* < 0.05.

cating a decrease in energy expenditure and heat production consistent with what we found previously.

To further explore this discrepancy in body weight phenotype as a result of housing temperature, we measured the CBT of *CREB1$^{\Delta SIM1}$* and control mice. *CREB1$^{\Delta SIM1}$* mice have a significantly lower CBT compared with controls, especially in the

evening (Fig. 4*C*). To further confirm this, we performed a cold challenge test in which CBT, body weight, and food intake were monitored for 7 h at 4 °C. *CREB1$^{\Delta SIM1}$* mice have a lower CBT during the first 3 h of cold exposure (CE) compared with controls (Fig. 4*D*). After 3 h of cold exposure, *CREB1$^{\Delta SIM1}$* mice recover their body temperature, which remains normal until
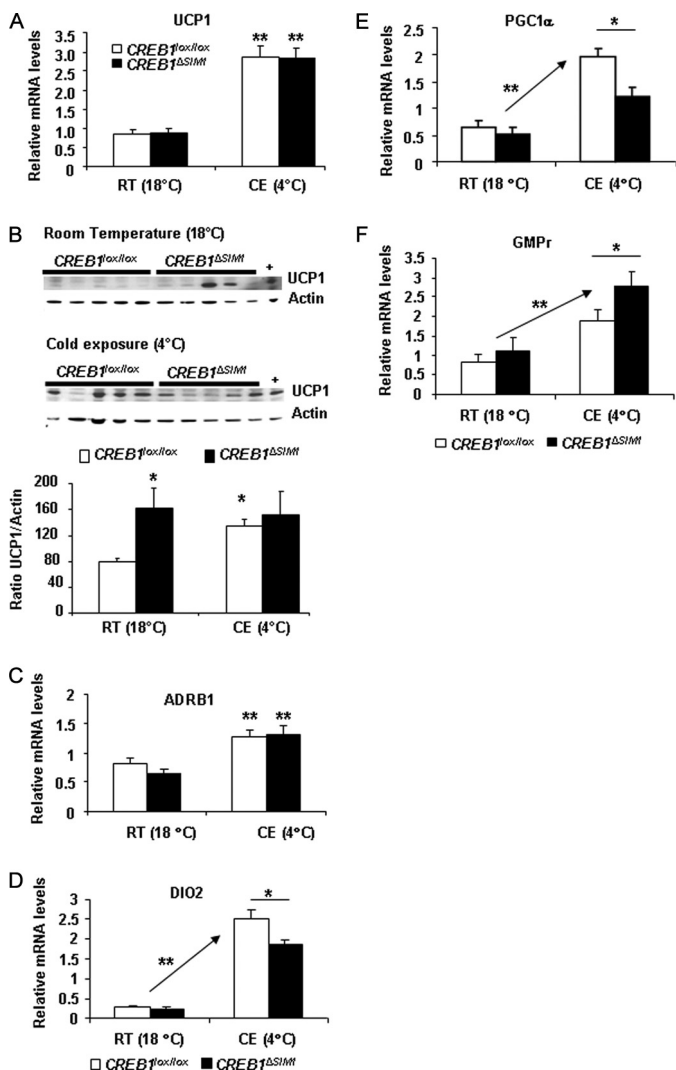
FIGURE 5. **Impaired BAT activation in *CREB1*$^{\Delta SIM1}$ mice.** *A*, uncoupling protein 1 (*UCP1*) relative mRNA expression at room temperature (18 °C) or after 7 h of CE at 4 °C. *B*, Western analysis and its quantification of UCP1 and actin at room temperature (*RT*, 18 °C) or after 7 h of CE at 4 °C. +, positive control; BAT from control mice after cold exposure. *C–F*, β-adrenergic 1 receptor (*ADRB1*) (*C*), *DIO2* (*D*), *PGC1α* (*E*), *GMPr* (*F*) relative mRNA expression, at room temperature (18 °C) or after 7 h of CE at 4 °C. The data are represented as the means ± S.E. At room temperature 18 °C, *n* = 8 mice/group; during cold exposure 4 °C, *n* = 7–8 mice/group. *, *p* < 0.05; **, *p* < 0.005.

the end of the experiment. Whereas both *CREB1*$^{\Delta SIM1}$ and control mice increase their food intake during cold exposure (supplemental Fig. S3*A*), only *CREB1*$^{\Delta SIM1}$ mice lose significant weight, indicating the increased energy cost of maintaining body temperature (supplemental Fig. S3*B*).

Taken together, these data demonstrate that *CREB1*$^{\Delta SIM1}$ mice at 22 °C have decreased energy expenditure, explaining the development of obesity on chow and high fat diets. At lower temperatures, *CREB1*$^{\Delta SIM1}$ mice must expend more energy to maintain their normal CBT, which induces weight loss.

CREB1$^{\Delta SIM1}$ *Mice Have a Defect in Brown Adipose Tissue*—To further determine how differences in temperature homeostasis may occur, we examined *UCP1* mRNA and protein expression as an indicator of brown adipose tissue (BAT) activation. *UCP1* mRNA was equally increased in both control and *CREB1*$^{\Delta SIM1}$ mice in response to CE (Fig. 5*A*). However, UCP1

protein expression is more abundant in *CREB1*$^{\Delta SIM1}$ mice at baseline and does not respond further to the CE, suggesting that *CREB1*$^{\Delta SIM1}$ mice cannot activate BAT in response to severe CE (Fig. 5*B*).

We next examined the expression of a number of genes involved in BAT function including *ACC1*, *DIO2*, *PGC1α*, *GMPr*, and *ADRB1*. As expected, both control and *CREB1*$^{\Delta SIM1}$ mice had increased expression of *ADRB1* consistent with sympathetic activation of BAT after CE (Fig. 5*C*). No change in *ADRB3* expression was observed (data not shown). However, expression of *DIO2* and *PGC1α* was significantly decreased in *CREB1*$^{\Delta SIM1}$ mice after CE, whereas *GMPr* gene expression was enhanced after CE (Fig. 5, *D–F*) (48). *UCP2* gene expression did not change between control and *CREB1*$^{\Delta SIM1}$ mice after CE (data not shown). Importantly, *creb1* mRNA expression in BAT is not modified in *CREB1*$^{\Delta SIM1}$ mice (data not shown). Thus *CREB1*$^{\Delta SIM1}$ mice have a defect in responding to CE despite enhanced sympathetic stimulation.

The impaired ability of the sympathetic nervous system in *CREB1*$^{\Delta SIM1}$ to stimulate BAT mice is supported by the gene expression patterns of these mice on HFD. Here, *CREB1*$^{\Delta SIM1}$ mice showed slightly increased *Adrb1* expression (supplemental Fig. S4*A*) and significantly decreased *GMPr* expression (supplemental Fig. S4*B*), suggesting impaired sympathetic activation. This is supported by increased *ACC1* expression (supplemental Fig. S4*C*), which is a marker of fatty acid synthesis. The exact mechanism underlying the defect remains to be fully characterized because *UCP1*, *DIO2*, and *PGC1α* are all equally expressed in control and *CREB1*$^{\Delta SIM1}$ mice on HFD (supplemental Fig. S4, *D–F*).

Disruption of CREB1 Does Not Impair the MC4R Pathway— Because the MC4R is expressed in *SIM1*-positive neurons and CREB1 has been hypothesized to be phosphorylated in MC4R-positive neurons in the PVN (37), we analyzed the MC4R pathway in *CREB1*$^{\Delta SIM1}$ mice. *In situ* hybridization of *MC4R* mRNA shows similar expression in control and *CREB1*$^{\Delta SIM1}$ mice, demonstrating that CREB1 is not required for *MC4R* expression (Fig. 6*A*). In addition, we pharmacologically tested the melanocortin pathway in *CREB1*$^{\Delta SIM1}$ lean mice by using two different analogues of α-MSH, the first specific to MC3/4Rs, MT II, and the second specific only to the MC4R, Ro27-3225. Compared with saline, both male and female control and *CREB1*$^{\Delta SIM1}$ mice showed a similar decline in food intake 3.5 h after injection of either MT II or Ro27-3225 (Fig. 6, *B* and *C*). Thus MC4R signaling as it relates to food intake appears to be normal in *CREB1*$^{\Delta SIM1}$ mice, which is consistent with the lack of hyperphagia seen in obese *CREB1*$^{\Delta SIM1}$ mice.

The Hypothalamic-Pituitary-Thyroid and -Adrenal Axes Are Normal in CREB1$^{\Delta SIM1}$ *Mice*—To evaluate the function of neuroendocrine circuits emanating from the PVN, we first looked at *TRH* mRNA expression in control and *CREB1*$^{\Delta SIM1}$ mice. *TRH* mRNA expression is enhanced in *CREB1*$^{\Delta SIM1}$ mice compared with control mice (Fig. 7*A*). In contrast, serum T4 levels were similar in control and *CREB1*$^{\Delta SIM1}$ mice fed a chow diet at 22 °C (Fig. 7*B*). Because thyroid hormone can participate in the maintenance of CBT, we also assessed the total T4 and total T3 serum levels in control and *CREB1*$^{\Delta SIM1}$ mice after 7 h of cold exposure (4 °C) and again saw no difference (Fig. 7, *C* and *D*).
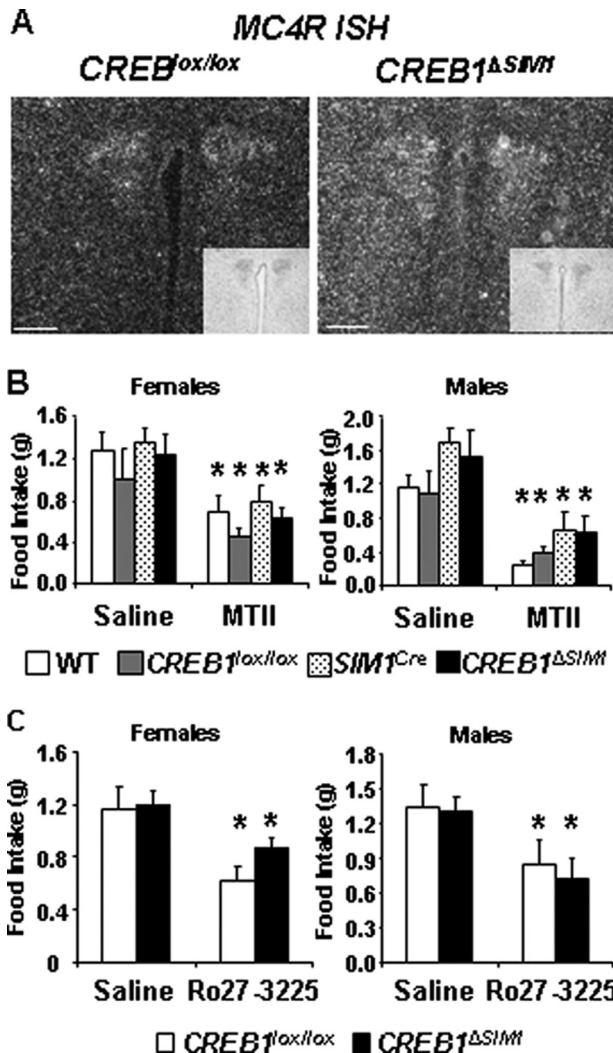
FIGURE 6. **The MC4R pathway is not affected by the lack of CREB1.** *A*, *in situ* hybridization of *MC4R* mRNA expression (dark field) and thionin staining (*inset*). *Bar scale*, 100 μm. Representative images from a total of three animals/ group. *B*, MT II test. After 12 h of fasting, saline (day 1) or MT II (day 2) was injected, and food intake was measured over a 3.5-h period. For n = males/ females: WT, $n = 8/8$; *CREB1*$^{lox/lox}$, $n = 8/8$; *SIM1*^{Cre}, $n = 6/8$; *CREB1*$^{\Delta SIM1}$ $n = 8/9$. *C*, Ro27-3225 Test. After 12 h of fasting, saline (day 1) or Ro27-3225 (day 2) was injected, and food intake was measured over a 3.5-h period. The data are represented as the means $\pm$ S.E. For n = males/females: *CREB1*$^{lox/lox}$, $n = 5/7$; *CREB1*$^{\Delta SIM1}$, $n = 8/8$. *, $p < 0.05$.

We also did not see differences in serum corticosterone levels in control and *CREB1*$^{\Delta SIM1}$ mice fed a chow diet at 22 °C (Fig. 7*E*). These data suggest that the decrease in energy expenditure and CBT observed in *CREB1*$^{\Delta SIM1}$ mice is not due to global alterations in the hypothalamic-pituitary-thyroid and hypothalamic-pituitary-adrenal axes.

CREB1$^{\Delta SIM1}$ *Mice Have a Decrease of AVP but Not OXT in the PVN*—Although both the thyroid and adrenal axis appeared normal, we next examined the expression of OXT and AVP, which are produced in MC4R- and SIM1-positive neurons in the PVN. OXT and AVP have been hypothesized to play a protective role in the prevention of obesity (14, 15). To accomplish, this we used quantitative immunohistochemistry to determine their abundance in the PVN. Whereas OXT levels were similar in control and *CREB1*$^{\Delta SIM1}$ mice (Fig. 8, *A* and *B*), AVP production was significantly reduced in the PVN (Fig. 8*C*).
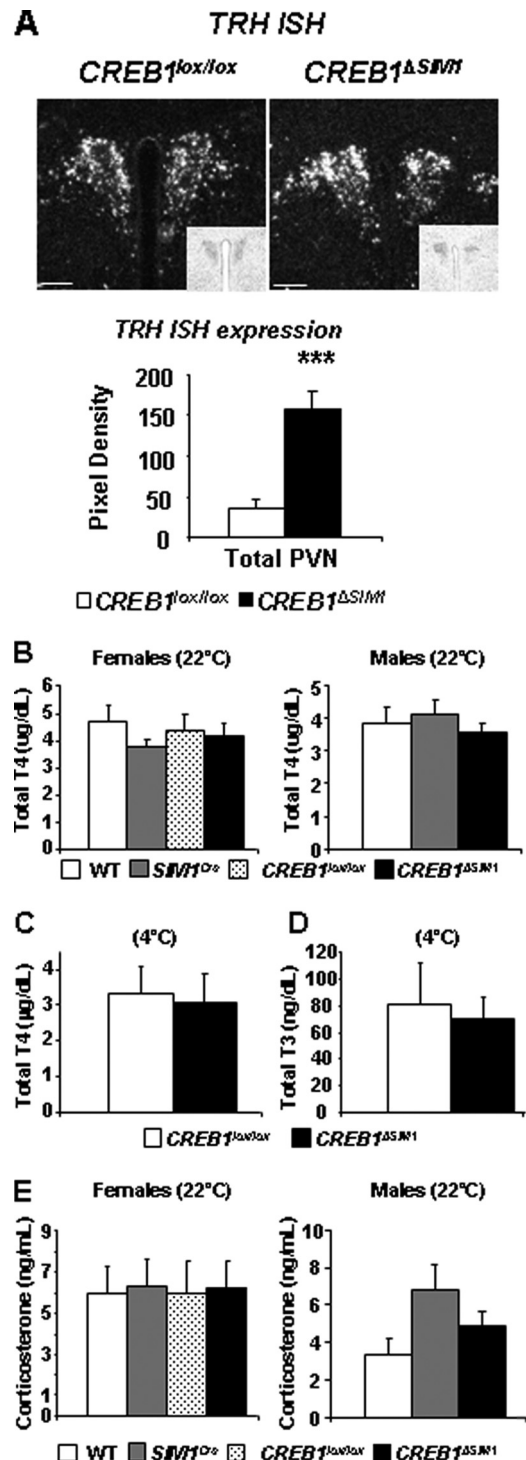
FIGURE 7. **CREB1**$^{\Delta SIM1}$ **mice have normal endocrine function.** *A*, *in situ* hybridization for TRH was performed in *CREB1*$^{lox/lox}$ and *CREB1*$^{\Delta SIM1}$ mice and subsequently quantified ($n = 5$). *B*, total T4 at 22 °C. *C* and *D*, total T4 (*C*) and total T3 (*D*) after 7 h at 4 °C ($n = 8$/group). *E*, corticosterone serum levels in male and female mice at 33 weeks of age on a chow diet. The data are represented as the means $\pm$ S.E. For n = males/females: WT, $n = 10/8$, *CREB1*$^{lox/lox}$, $n = 12/12$, *SIM1*^{Cre}, $n = 6$ males; *CREB1*$^{\Delta SIM1}$, $n = 11/13$.

A more careful analysis of the different subpopulations of neurons in the PVN (Fig. 8*D*) demonstrates that the anterior parvicellular, medial magnocellular, and medial parvicellular nuclei are most affected. Because OXT and AVP are also expressed in the SON, we quantified their expression in this
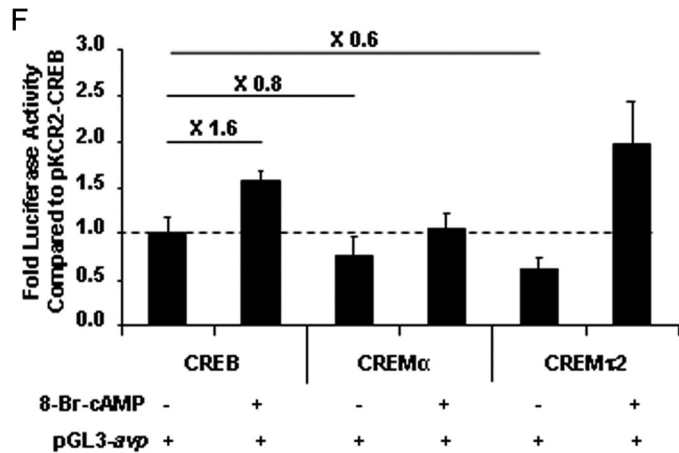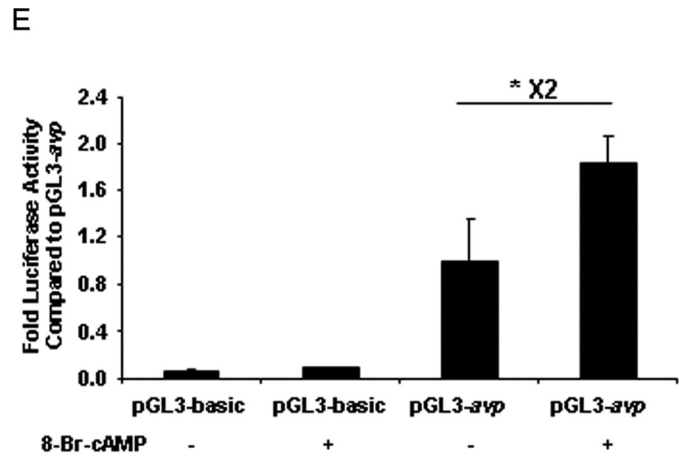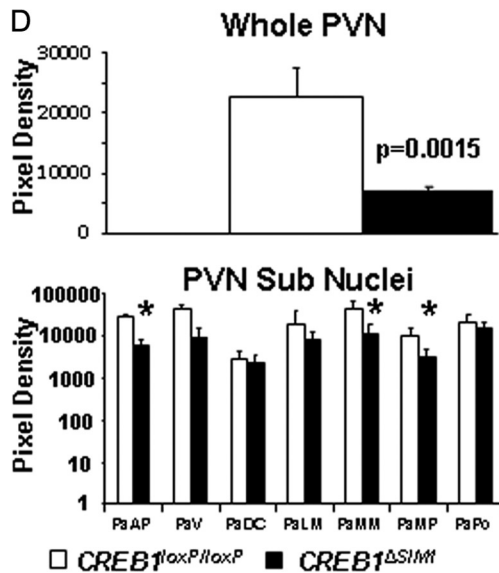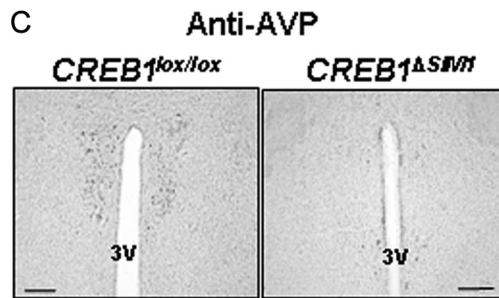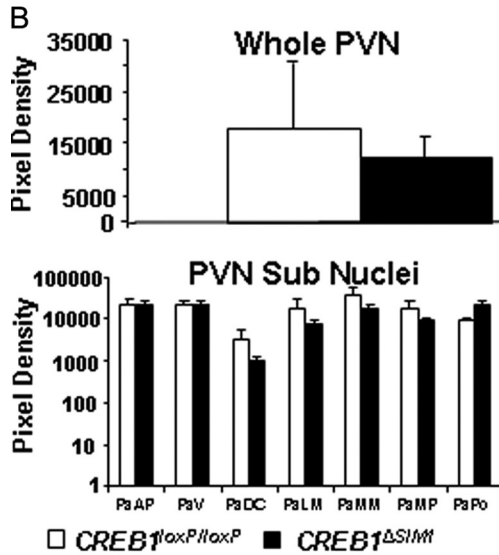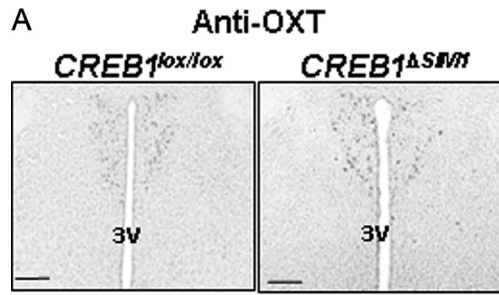
area and observed no difference between control and *CREB1*$^{\Delta SIM1}$ mice (supplemental Fig. S5, *A–D*).

To confirm that AVP expression could be influenced by the cAMP-CREB pathway, we cloned the murine AVP promoter upstream of luciferase and tested its activity in 293T cells. Indeed, 8-bromo-cAMP was able to stimulate expression of luciferase, consistent with what has been described previously with the AVP rat promoter (Fig. 8*E*) (49). Interestingly, when we cotransfected two isoforms of CREM, we observed a significant repression of luciferase activity when compared with cotransfected CREB1 (Fig. 8*F*). The cotransfection of CREM isoforms or CREB1 did not affect cAMP stimulation (Fig. 8*F*).

DISCUSSION

CREB1 is a transcription factor that can drive the expression of numerous genes (27, 50) implicated in the regulation of food intake and energy expenditure including TRH, CRH, OXT, and AVP (14, 15, 51–53). In addition, CREB1 has been postulated to play a key role downstream of the MC4R in the PVN (37). Thus to test the role of CREB1 in body weight regulation and MC4R signaling, we chose to delete CREB1 from *SIM1*-positive neurons in the PVN using a conditional targeting strategy. Indeed, all MC4R neurons in the PVN express SIM1 (16). However, because *SIM1* is also expressed in other neuronal groups, we deleted CREB1 in the NLOT, SON, and MeAD. A PVN-only specific *Cre* currently does not exist, making this the best available strategy to test the role of CREB1 in a unique set of neurons known to regulate body weight.

Importantly, we have established that the deletion of CREB1 from the PVN does not impair the integrity of these neurons. Lack of CREB1, CREM, or both can induce apoptosis and neurodegeneration as described previously (26, 28–30). However, by deleting CREB1, we have clearly up-regulated CREM expression, which could potentially compensate for the lack of CREB1. Thus this model may under-represent the importance of the CREB family in body weight regulation. The third member of the CREB family, activating transcription factor 1 does not appear to be expressed in the murine brain (54).

By deleting CREB1 in neurons where *SIM1* is expressed, we found that obesity was induced provided the animals were housed at warmer temperatures (22 °C). Surprisingly, this obesity was not the result of increased food intake but was secondary to decreased energy expenditure. Furthermore, glucose intolerance in these mice was relatively mild despite the development of obesity. Mice that lack $G_s\alpha$ in the brain develop a similar phenotype (55). Indeed, $G_s\alpha$ lies immediately downstream of the MC4R and is proximal to CREB1. Disruption of the maternal (but not paternal) $G_s\alpha$ allele in the brain leads to the development of obesity, insulin resistance, and diabetes associated with reduced sympathetic nervous system activity and energy expenditure (56). This appears to be primarily due to a lack of $G_s\alpha$ in the PVN. Similar to our model, these animals had no evidence of hyperphagia. These data suggest that the PKA-CREB1 pathway may be important in the regulation of energy expenditure by the MC4R. In contrast, our pharmacologic data clearly show that CREB1 is not required for the regulation of food intake by the MC4R. Thus it remains possible that MC4R is able to signal through other non-PKA/CREB pathways such as the MAPK pathway or through the EPACs (exchange proteins directly activated by cAMP). These pathways have been linked to both the MC4R and cAMP signaling (57–59).

Another striking finding in *CREB1*$^{\Delta SIM1}$ mice is that development of obesity is prevented when they are housed at colder temperatures. Because *CREB1*$^{\Delta SIM1}$ mice have a defect in BAT-mediated adaptive thermogenesis, they must evoke other thermogenic mechanisms that are less efficient and therefore lead to an increase in energy expenditure when housed in the cold. Previous work has demonstrated that the MC4R plays a critical role in energy homeostasis and regulation of adaptive thermogenesis by activating UCP1 in BAT through the sympathetic nervous system (7, 60, 61). Consistent with this, *CREB1*$^{\Delta SIM1}$ mice are unable to further activate UCP1 protein levels in response to a cold challenge indicative of a deficit in BAT activation. Impairment of *PGC1α* and *DIO2* induction in BAT of *CREB1*$^{\Delta SIM1}$ mice during a cold challenge despite their enhanced sympathetic stimulation further supports this hypothesis. Indeed, the PVN, which contains SIM1 and AVP immunoreactive positive neurons, projects to the dorsal vagal complex, as well as to sympathetic centers located in the spinal cord (62–66). Because AVP expression is decreased in our mouse model, this could explain why sympathetic nervous system function is altered. Taken together, the data suggest that CREB signaling in the PVN regulates body weight by altering energy expenditure potentially through the sympathetic nervous system and possibly the MC4R, which has been shown to affect this pathway when activated.

Finally, our work demonstrates that obese *CREB1*$^{\Delta SIM1}$ mice have altered AVP protein expression in the PVN but not in the SON, implicating AVP in the phenotype of *CREB1*$^{\Delta SIM1}$ mice. Indeed, the AVP promoter contains two CRE sites (49, 67) and responds to cAMP in our transfection system. Additionally, down-regulation of AVP is associated with the development of obesity (11, 14, 42, 68). Essentially, AVP appears to be specifically targeted in *CREB1*$^{\Delta SIM1}$ mice because the regulation of other key PVN-specific neuropeptides and the pathways they control are unaffected. Further work will be required to deter-

---

FIGURE 8. ***CREB1*$^{\Delta SIM1}$ mice have decreased in AVP expression.** *A*, immunohistochemistry for OXT in *CREB1*$^{lox/lox}$ and *CREB1*$^{\Delta SIM1}$ mice. *B*, quantification of OXT immunohistochemistry in *CREB1*$^{lox/lox}$ and *CREB1*$^{\Delta SIM1}$ mice. *C*, immunohistochemistry for AVP in *CREB1*$^{lox/lox}$ and *CREB1*$^{\Delta SIM1}$ mice. *D*, quantification of AVP expression in *CREB1*$^{lox/lox}$ and *CREB1*$^{\Delta SIM1}$ brains. The data represent the pixel density in whole PVN and in the different subnuclei of the PVN and are expressed as the means ± S.E. *, $p < 0.05$. The mice were 33 weeks old, fed with chow diet, and housed at 22 °C ($n = 4$/group). *PaAP*, paraventricular hypothalamic nucleus, anterior parvicellular part; *PaDC*, paraventricular hypothalamic nucleus, dorsal cap; *PaLM*, paraventricular hypothalamic nucleus, lateral magnocellular part; *PaMM*, paraventricular hypothalamic nucleus, medial magnocellular part; *PaMP*, paraventricular hypothalamic nucleus, medial parvicellular part; *PaPo*, paraventricular hypothalamic nucleus, posterior part; *PaV*, paraventricular hypothalamic nucleus, ventral part; *3V*, third ventricle. *Bar scale*, 100 μm. *E*, 293T cells were transfected with either pGL3 AVP-luc or pGL3-luc alone and a CMV-β galactosidase control. *, $p < 0.05$. *F*, 293T-cells were cotransfected with AVP-Luc, a CMV-β galactosidase control, and either pKCR2-CREB, pKCR2-CREMα, or pCDNA3.1-CREMτ2 in the presence or absence of 250 μM 8-bromo-cAMP (*8-Br-cAMP*).

mine the role of AVP in the phenotype seen in *CREB1*$^{\Delta SIM1}$ mice.

In summary, we demonstrate that disruption of CREB1 in SIM1-positive neurons led to an obese phenotype similar to that of the PVN-specific G$_s\alpha$ knock-out mice. Our findings clearly underline the value of the PKA-CREB1 pathway in the regulation of body weight. However, the phenotype of both *CREB1*$^{\Delta SIM1}$ mice and G$_s\alpha$ knock-out mice is milder and distinct from both the MC4R knock-out mouse and the SIM1 haploinsufficient mouse. This suggests that the MC4R may only partially signal through the PKA-CREB1 pathway in the PVN to mediate its effects.

REFERENCES

1. Kishi, T., Aschkenasi, C. J., Lee, C. E., Mountjoy, K. G., Saper, C. B., and Elmquist, J. K. (2003) *J. Comp. Neurol.* **457,** 213–235
2. Liu, H., Kishi, T., Roseberry, A. G., Cai, X., Lee, C. E., Montez, J. M., Friedman, J. M., and Elmquist, J. K. (2003) *J. Neurosci.* **23,** 7143–7154
3. Mountjoy, K. G., Mortrud, M. T., Low, M. J., Simerly, R. B., and Cone, R. D. (1994) *Mol. Endocrinol.* **8,** 1298–1308
4. Huszar, D., Lynch, C. A., Fairchild-Huntress, V., Dunmore, J. H., Fang, Q., Berkemeier, L. R., Gu, W., Kesterson, R. A., Boston, B. A., Cone, R. D., Smith, F. J., Campfield, L. A., Burn, P., and Lee, F. (1997) *Cell* **88,** 131–141
5. Yeo, G. S., Farooqi, I. S., Challis, B. G., Jackson, R. S., and O'Rahilly, S. (2000) *Q. J. Med.* **93,** 7–14
6. Chen, A. S., Metzger, J. M., Trumbauer, M. E., Guan, X. M., Yu, H., Frazier, E. G., Marsh, D. J., Forrest, M. J., Gopal-Truter, S., Fisher, J., Camacho, R. E., Strack, A. M., Mellin, T. N., MacIntyre, D. E., Chen, H. Y., and Van der Ploeg, L. H. (2000) *Transgenic Res.* **9,** 145–154
7. Ste Marie, L., Miura, G. I., Marsh, D. J., Yagaloff, K., and Palmiter, R. D. (2000) *Proc. Natl. Acad. Sci. U.S.A.* **97,** 12339–12344
8. Balthasar, N. (2006) *Obesity* **14,** (Suppl. 5) 222S–227S
9. Hollenberg, A. N. (2008) *Thyroid* **18,** 131–139
10. Lechan, R. M., and Fekete, C. (2006) *Peptides* **27,** 310–325
11. Valassi, E., Scacchi, M., and Cavagnini, F. (2008) *Nutr. Metab. Cardiovasc. Dis.* **18,** 158–168
12. Balthasar, N., Dalgaard, L. T., Lee, C. E., Yu, J., Funahashi, H., Williams, T., Ferreira, M., Tang, V., McGovern, R. A., Kenny, C. D., Christiansen, L. M., Edelstein, E., Choi, B., Boss, O., Aschkenasi, C., Zhang, C. Y., Mountjoy, K., Kishi, T., Elmquist, J. K., and Lowell, B. B. (2005) *Cell* **123,** 493–505
13. Holder, J. L., Jr., Butte, N. F., and Zinn, A. R. (2000) *Hum. Mol. Genet.* **9,** 101–108
14. Kublaoui, B. M., Gemelli, T., Tolson, K. P., Wang, Y., and Zinn, A. R. (2008) *Mol. Endocrinol.* **22,** 1723–1734
15. Kublaoui, B. M., Holder, J. L., Jr., Gemelli, T., and Zinn, A. R. (2006) *Mol. Endocrinol.* **20,** 2483–2492
16. Michaud, J. L., Boucher, F., Melnyk, A., Gauthier, F., Goshu, E., Lévy, E., Mitchell, G. A., Himms-Hagen, J., and Fan, C. M. (2001) *Hum. Mol. Genet.* **10,** 1465–1473
17. Yang, Y., Gagnon, D., Vachon, P., Tremblay, A., Levy, E., Massie, B., and Michaud, J. L. (2006) *J. Neurosci.* **26,** 7116–7120
18. Lee, E. J., Lee, S. H., Jung, J. W., Lee, W., Kim, B. J., Park, K. W., Lim, S. K., Yoon, C. J., and Baik, J. H. (2001) *Eur. J. Biochem.* **268,** 582–591
19. Haus-Seuffert, P., and Meisterernst, M. (2000) *Mol. Cell Biochem.* **212,** 5–9
20. Johannessen, M., Delghandi, M. P., and Moens, U. (2004) *Cell Signal* **16,** 1211–1227
21. Mayr, B., and Montminy, M. (2001) *Nat. Rev. Mol. Cell Biol.* **2,** 599–609
22. Sassone-Corsi, P. (1998) *Int. J. Biochem. Cell Biol.* **30,** 27–38
23. Czyzyk, T. A., Sikorski, M. A., Yang, L., and McKnight, G. S. (2008) *Proc. Natl. Acad. Sci. U.S.A.* **105,** 276–281
24. Impey, S., McCorkle, S. R., Cha-Molstad, H., Dwyer, J. M., Yochum, G. S., Boss, J. M., McWeeney, S., Dunn, J. J., Mandel, G., and Goodman, R. H. (2004) *Cell* **119,** 1041–1054
25. Lonze, B. E., and Ginty, D. D. (2002) *Neuron* **35,** 605–623
26. Bleckmann, S. C., Blendy, J. A., Rudolph, D., Monaghan, A. P., Schmid, W., and Schütz, G. (2002) *Mol. Cell. Biol.* **22,** 1919–1925
27. Blendy, J. A., Kaestner, K. H., Schmid, W., Gass, P., and Schutz, G. (1996) *EMBO J.* **15,** 1098–1106
28. Mantamadiotis, T., Lemberger, T., Bleckmann, S. C., Kern, H., Kretz, O., Martin Villalba, A., Tronche, F., Kellendonk, C., Gau, D., Kapfhammer, J., Otto, C., Schmid, W., and Schütz, G. (2002) *Nat. Genet.* **31,** 47–54
29. Parlato, R., Otto, C., Begus, Y., Stotz, S., and Schütz, G. (2007) *Development* **134,** 1663–1670
30. Parlato, R., Rieker, C., Turiault, M., Tronche, F., and Schütz, G. (2006) *Genesis* **44,** 454–464
31. Ruppert, S., Cole, T. J., Boshart, M., Schmid, E., and Schütz, G. (1992) *EMBO J.* **11,** 1503–1512
32. Conkright, M. D., Canettieri, G., Screaton, R., Guzman, E., Miraglia, L., Hogenesch, J. B., and Montminy, M. (2003) *Mol. Cell* **12,** 413–423
33. Lerner, R. G., Depatie, C., Rutter, G. A., Screaton, R. A., and Balthasar, N. (2009) *EMBO Rep.* **10,** 1175–1181
34. Altarejos, J. Y., Goebel, N., Conkright, M. D., Inoue, H., Xie, J., Arias, C. M., Sawchenko, P. E., and Montminy, M. (2008) *Nat. Med.* **14,** 1112–1117
35. Harris, M., Aschkenasi, C., Elias, C. F., Chandrankunnel, A., Nillni, E. A., Bjøorbaek, C., Elmquist, J. K., Flier, J. S., and Hollenberg, A. N. (2001) *J. Clin. Invest.* **107,** 111–120
36. Selkirk, J. V., Nottebaum, L. M., Ford, I. C., Santos, M., Malany, S., Foster, A. C., and Lechner, S. M. (2006) *J. Biomol. Screen* **11,** 351–358
37. Sarkar, S., Légrádi, G., and Lechan, R. M. (2002) *Brain Res.* **945,** 50–59
38. Mantamadiotis, T., Kretz, O., Ridder, S., Bleckmann, S. C., Bock, D., Gröne, H. J., Malaterre, J., Dworkin, S., Ramsay, R. G., and Schütz, G. (2006) *Mol. Endocrinol.* **20,** 204–211
39. Sugrue, M. L., Vella, K. R., Morales, C., Lopez, M. E., and Hollenberg, A. N. (2009) *Endocrinology* **151,** 793–801
40. Gross, D. S., and Rothfeld, J. M. (1985) *J. Histochem. Cytochem.* **33,** 11–20
41. Itoi, K., Jiang, Y. Q., Iwasaki, Y., and Watson, S. J. (2004) *J. Neuroendocrinol.* **16,** 348–355
42. Kiss, J. Z., Mezey, E., and Skirboll, L. (1984) *Proc. Natl. Acad. Sci. U.S.A.* **81,** 1854–1858
43. Kovács, K. J., and Sawchenko, P. E. (1996) *J. Neurosci.* **16,** 262–273
44. Kublaoui, B. M., Holder, J. L., Jr., Tolson, K. P., Gemelli, T., and Zinn, A. R. (2006) *Endocrinology* **147,** 4542–4549
45. Vella, K. R., Burnside, A. S., Brennan, K. M., and Good, D. J. (2007) *J. Neuroendocrinol.* **19,** 499–510
46. Benoit, S. C., Schwartz, M. W., Lachey, J. L., Hagan, M. M., Rushing, P. A., Blake, K. A., Yagaloff, K. A., Kurylko, G., Franco, L., Danhoo, W., and Seeley, R. J. (2000) *J. Neurosci.* **20,** 3442–3448
47. Segal-Lieberman, G., Bradley, R. L., Kokkotou, E., Carlson, M., Trombly, D. J., Wang, X., Bates, S., Myers, M. G., Jr., Flier, J. S., and Maratos-Flier, E. (2003) *Proc. Natl. Acad. Sci. U.S.A.* **100,** 10085–10090
48. Christoffolete, M. A., Linardi, C. C., de Jesus, L., Ebina, K. N., Carvalho, S. D., Ribeiro, M. O., Rabelo, R., Curcio, C., Martins, L., Kimura, E. T., and Bianco, A. C. (2004) *Diabetes* **53,** 577–584
49. Iwasaki, Y., Oiso, Y., Saito, H., and Majzoub, J. A. (1997) *Endocrinology* **138,** 5266–5274
50. Cha-Molstad, H., Keller, D. M., Yochum, G. S., Impey, S., and Goodman, R. H. (2004) *Proc. Natl. Acad. Sci. U.S.A.* **101,** 13572–13577
51. Lechan, R. M., and Fekete, C. (2006) *Prog. Brain Res.* **153,** 209–235
52. Nieuwenhuizen, A. G., and Rutters, F. (2008) *Physiol. Behav.* **94,** 169–177
53. Duan, J., Choi, Y. H., Hartzell, D., Della-Fera, M. A., Hamrick, M., and Baile, C. A. (2007) *Obesity* **15,** 2624–2633
54. Hummler, E., Cole, T. J., Blendy, J. A., Ganss, R., Aguzzi, A., Schmid, W., Beermann, F., and Schütz, G. (1994) *Proc. Natl. Acad. Sci. U.S.A.* **91,** 5647–5651

55. Chen, M., Wang, J., Dickerson, K. E., Kelleher, J., Xie, T., Gupta, D., Lai, E. W., Pacak, K., Gavrilova, O., and Weinstein, L. S. (2009) *Cell Metab.* **9,** 548–555

56. Xie, T., Chen, M., Gavrilova, O., Lai, E. W., Liu, J., and Weinstein, L. S. (2008) *Endocrinology* **149,** 2443–2450

57. Daniels, D., Patten, C. S., Roth, J. D., Yee, D. K., and Fluharty, S. J. (2003) *Brain Res.* **986,** 1–11

58. Kawasaki, H., Springett, G. M., Mochizuki, N., Toki, S., Nakaya, M., Matsuda, M., Housman, D. E., and Graybiel, A. M. (1998) *Science* **282,** 2275–2279

59. Patten, C. S., Daniels, D., Suzuki, A., Fluharty, S. J., and Yee, D. K. (2007) *Regul. Pept.* **142,** 111–122

60. Voss-Andreae, A., Murphy, J. G., Ellacott, K. L., Stuart, R. C., Nillni, E. A., Cone, R. D., and Fan, W. (2007) *Endocrinology* **148,** 1550–1560

61. Fan, W., Voss-Andreae, A., Cao, W. H., and Morrison, S. F. (2005) *Peptides* **26,** 1800–1813

62. Duplan, S. M., Boucher, F., Alexandrov, L., and Michaud, J. L. (2009) *Eur. J. Neurosci.* **30,** 2239–2249

63. Saper, C. B., Loewy, A. D., Swanson, L. W., and Cowan, W. M. (1976) *Brain Res.* **117,** 305–312

64. Sawchenko, P. E. (1998) *J. Comp. Neurol.* **402,** 435–441

65. Sawchenko, P. E., and Swanson, L. W. (1982) *Brain Res.* **257,** 275–325

66. Swanson, L. W., and Kuypers, H. G. (1980) *J. Comp. Neurol.* **194,** 555–570

67. Kuwahara, S., Arima, H., Banno, R., Sato, I., Kondo, N., and Oiso, Y. (2003) *J. Neurosci.* **23,** 10231–10237

68. Caldwell, H. K., Lee, H. J., Macbeth, A. H., and Young, W. S., 3rd (2008) *Prog. Neurobiol.* **84,** 1–24